8-10-1998

Production of Energy-dependent Time Delays in Impulsive Solar Flare Hard X-Ray Emission by Short-Duration Spectral Index Variations

Ted N. La Rosa
Kennesaw State University, tlarosa1@kennesaw.edu

Steven N. Shore
Indiana University - South Bend

Recommended Citation

LaRosa TN and Shore SN. 1998. Production of energy-dependent time delays in impulsive solar flare hard X-ray emission by short-duration spectral index variations. Astrophys J 503(1):429-34.

THE ASTROPHYSICAL JOURNAL, 503:429–434, 1998 August 10

PRODUCTION OF ENERGY-DEPENDENT TIME DELAYS IN IMPULSIVE SOLAR FLARE HARD X-RAY EMISSION BY SHORT-DURATION SPECTRAL INDEX VARIATIONS

T. N. LAROSA
Department of Biological and Physical Sciences, Kennesaw State University, 1000 Chastain Road, Kennesaw, GA 30144
AND
STEVEN N. SHORE
Department of Physics and Astronomy, Indiana University South Bend, 1700 Mishawaka Avenue, South Bend, IN 46634-7111
Received 1997 December 23; accepted 1998 March 16

ABSTRACT

Cross-correlation techniques have been used recently to study the relative timing of solar flare hard X-ray emission at different energies. These studies find that for the majority of the impulsive flares observed with BATSE there is a systematic time delay of a few tens of milliseconds between low (≈ 50 keV) and higher energy emission (≈ 100 keV). These time delays have been interpreted as energy-dependent time-of-flight differences for electron propagation from the corona, where they are accelerated, to the chromosphere, where the bulk of the hard X-rays are emitted. We show in this paper that cross-correlation methods fail if the spectral index of the flare is not constant. BATSE channel ratios typically display variations of factors of 2 to 5 over time intervals as short as a few seconds. Using simulated and observed data, we demonstrate that cross-correlating energy channels with identical timing characteristics, but with variations in the amplitudes of one or a small number of relatively strong emission spikes, produces asymmetric time delays of either sign. The reported time delays are therefore largely due to spectral index variations and are not signatures of time-of-flight effects.
Subject headings: Sun: flares — Sun: X-rays, gamma rays — Sun: particle emission

1. INTRODUCTION

Impulsive hard X-ray emission produced by high-energy accelerated electrons is the primary signature of rapid energy release during solar flares. The number of electrons accelerated, their energy spectrum, and their timing are the most useful constraints for determining the mechanism(s) responsible for the rapid energy conversion taking place during a flare (for a recent comprehensive review see Miller et al. 1997). Recently, new high-sensitivity, high time resolution, hard X-ray observations, made with the Burst and Transient Source Experiment (BATSE) on board the *Compton Gamma Ray Observatory*, have provided the impetus for a number of studies on the timing of high- versus low-energy emission. Aschwanden & Schwartz (1996) and Aschwanden et al. (1996a, 1996b) have found that in the majority of impulsive flares, high-energy emission systematically precedes low-energy emission by tens of milliseconds. They interpret these time delays as the result of energy-dependent time-of-flight (TOF) differences for electrons propagating from a coronal acceleration site to the chromosphere. By combining the TOF results with hard X-ray images, it is possible to infer the location and the geometry of the flare acceleration site (Aschwanden et al. 1996a). These studies suggest that flare acceleration sites are located at the tops of loops in magnetic cusp regions. This result, if correct, is strong evidence in favor of reconnection models of solar flares (e.g., Hirayama 1974; Kopp & Pneuman 1976; Sturrock 1966; Tsuneta 1996).

The validity of the timing results depends on the applicability of correlation methods to the BATSE data. The fundamental underlying assumption is that the relative timing between energy channels is due solely to the time dependence of the emission and is independent of the amplitude of the emission as a function of energy. Our purpose in this paper is to demonstrate that amplitude variations are capable of producing the time delays derived from correlation analyses. Consequently, the time delays cannot be uniquely interpreted as being the result of TOF differences (LaRosa, Shore, & Zollistch 1997).

2. DATA ANALYSIS

We used two principal criteria to select the data discussed here. The first was to reanalyze a subset of flares discussed by Aschwanden et al. (1996a, hereafter A96a). These are the largest flares in the BATSE database for which contemporaneous *Yohkoh* images exist. The second was to select flares for which there exist complete medium energy resolution (MER) data sets. These data are burst triggered with 16 ms sampling that is rebinned to 64 ms resolution. A burst data set has 16 energy channels, each with 2560 points covering an interval of 164 s. These observations provide the highest time resolution and signal-to-noise ratio (for further discussion of the BATSE flare data see Aschwanden & Schwartz 1996). Table 1 lists the flares we have in common with A96a. For brevity, we present data only for those flares for which time delays have been previously published. A more complete analysis will be published separately.

2.1. *Procedures*

The hard X-ray light curves were analyzed in a three-step process. Figure 1 (*top left*) shows a typical flare light curve, in this case burst 1181, in two energy channels. This flare serves as our illustration of the procedure.

The first step is to separate the fast timescale variations from the slowly varying emission by digitally filtering the data. *Any* cross-correlation analysis of short-time variations, i.e., spikes, requires that all long-term variability first be removed from the data in order not to produce a spurious correlation. This is analogous to removing the season-

TABLE 1

RESULTS OF CORRELATION ANALYSIS

Flare Burst	Channel Number	Filter Width (s)	Spike Delay (ms)	Envelope Delay (ms)	A96a Filter Width (s)	A96a Spike Delay (ms)	A96a Envelope Delay (ms)
1032	3	10	37	−45	3.6	28	−100
	4	10	0	−59	3.6	34	−300
	5	10	−36	−56	3.6	51	−750
	6	10	−114	−158	3.6	43	−900
1037	3	10	21	366	2.5	13	1100
	4	10	28	808	2.5	51	2300
	5	10	32	1011	2.5	61	2400
	6	10	42	1076	2.5	76	2000
	7	10	62	1023	2.5	101	1400
	8	10	53	727	2.5	106	800
1066	3	10	58	−55	1.5	35	50
	4	10	78	−103	1.5	61	0
	5	10	106	−188	1.5	86	−25
	6	10	129	−285	1.5	114	−100
1146	3	10	49	−39	2	24	80
	4	10	102	−86	2	47	110
	5	10	157	−208	2	64	120
	6	10	251	−399	2	83	80
	7	10	365	−640	2	95	−100
1181	5	10	14	−117	3	18	−90
	6	10	26	−289	3	29	−170
	7	10	36	−486	3	40	−230
	8	10	49	−658	3	50	−380
	9	10	55	−961	3	60	−550
	10	10	66	−1304	3	70	−900
1227	3	10	2	407	1	18	−35
	4	10	10	475	1	36	−100
	5	10	8	517	1	37	−150
	6	10	9	530	1	57	−200
	7	10	25	590	1	66	−270

al trend from a time series analysis of weather or removing a filtered background in the analysis of turbulence in a molecular cloud (e.g., Miesch & Bally 1994). As in Aschwanden & Schwartz (1996), this is accomplished using a fast Fourier transform (FFT).[1] The resulting FFT for each channel is trimmed, Fourier inverted, and finally subtracted without scaling from the original data. This creates a high pass digital filter that admits variations only faster than a specified timescale, the filter width. In our analysis we used a *fixed* filter width of 10 s for all flares. This choice is motivated by the fact the power spectrum analyses indicate that nearly all flares in our study have well-defined emission peaks lasting of order 10–12 s. Filter widths of a few seconds or less produce correlation functions that are substantially reduced in signal-to-noise ratio. The filtered profiles for channels 4 and 7 are displayed in Figure 1 (*top left*), and the residual spike emission for channel 4, which is left after subtracting the filtered profile from the data in Figure 1 (*top right*), is displayed in Figure 1 (*bottom left*).

In the second step, the residuals from the different energy channels are auto- and cross-correlated. To continue with our illustration, the resulting auto- and cross-correlation functions for channels 4 and 7 are shown in Figure 1 (*bottom right*). We generally eliminated the first 200 data points to avoid edge effects in the filtering process. This is especially important for those flares caught already on the rise. The upper time limit to the range is set by the time at which the emission falls to background levels.

In the third step, we determine the peak of the correlation functions using a nonlinear least-squares Gaussian fitting routine. Table 1 gives our results for all flares in common with A96a. The first column lists the burst number, and the second column gives the MER channel that was correlated with the reference channel.[2] Our filter width was always 10 s and for reference is listed in the third column. The fourth and fifth columns list our results for the time delays between the spike emission and the slowly varying envelope emission. The published results are shown for comparison. The sixth column lists the filter width with which the A96a results were obtained, and the seventh and eighth columns list those published time delays.

2.2. *Derivation of Time Delays*

One basic result of our correlation analysis is its extreme sensitivity to the properties of the data set. Simply changing the length of the sampled interval, the starting and ending times, or the width of the filter changes the magnitude and/or sign of the time delay in unpredictable ways. Take, for example, burst 1296—the so-called Masuda flare—for which Aschwanden et al. (1996) report large energy-dependent delays (e.g., $+107 \pm 21$ ms for channel 3 delay with channel 5). Their delays were derived using a 32 s filter width using all 2560 points. Aschwanden & Schwartz (1996) found that filter width strongly affects the derived time delays. Here we point out that the derived delays are also strongly influenced by the portion of the data set selected

[1] These were computed for the individual energy channels using the FFT routine available in interactive data language (IDL).

[2] The reference channel number is always one less than the first value listed in the second column.

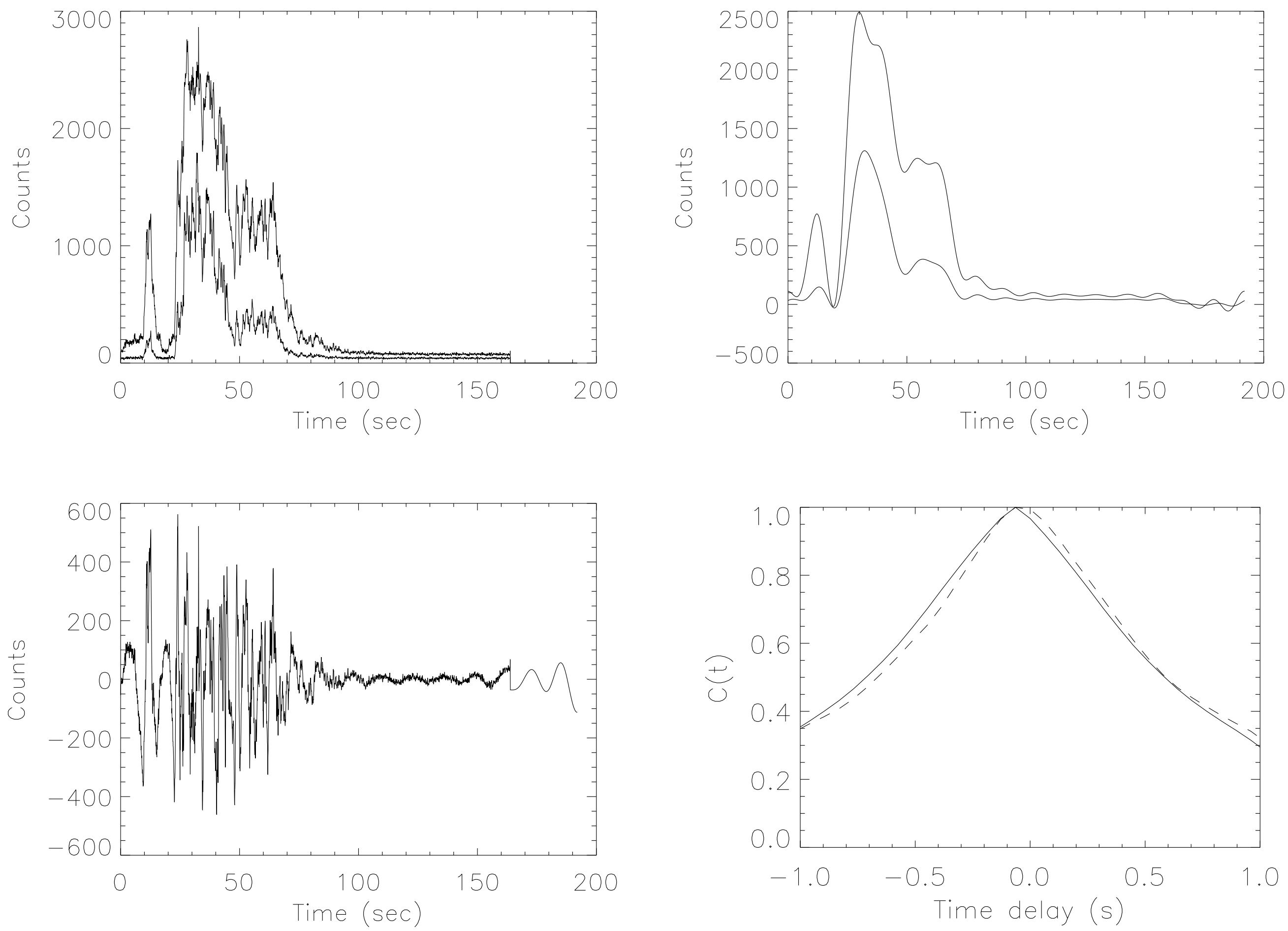

FIG. 1.—Example of correlation analysis for burst 1181 (1991 December 15, start time 18:32 UT). Hard X-ray light curves for MER channels 4 (41–54 keV) and 7 (97–122 keV) (*top left*). Filtered envelope profiles for data in top left panel obtained using an FFT with a 10 s filter (*top right*). Residual spike emission obtained by subtracting filtered envelope from observed data (*bottom left*). Autocorrelation function for channel 4 residuals (*solid line*) and cross-correlation of residuals of channels 4 and 7 (*bottom right, dashed line*). The plot shows the normalized correlation function vs. time lag (s). The spike at zero lag is due to the intrinsic noise in the data and must be present in any autocorrelation (see A96a).

for analysis. We again used a fixed filter width of 10 s and cross-correlated channels 3 and 5 using different portions of the time series. The use of points between 25 to 90 s only yields a time delay of −59 ms, the use of points from 25 to 102 s gives no delay, and the use of points 38 to 115 s yields a delay of +69 ms. *Notice that this last shift differs from the first by a factor of 2 in magnitude and has the opposite sign.* Similar results are obtained by cross-correlating channels 2 and 4: using all data points yields a +70 ms shift, but if we restrict the sample to points from 13 to 128 s, the shift is 4 times larger, i.e., 280 ms. Finally, using only the interval from 13 to 90 s yields a shift of +240 ms. It is therefore possible to derive a broad range of time delays with opposite directions of shift *from the same data set*.

We found the same result for the other flares in our sample. This calls into question the physical nature of the delays and suggests to us that they are an artifact of the analysis procedure.

2.3. *Spectral Index Variations*

We noticed that many flares in our sample show large spectral index changes. These occur on the long timescale, varying slowly over the course of the whole flare and, more importantly, within spikes on timescales as short as a few seconds. For example, Figure 2 shows several typical channel ratios for different flares. Note that changes in the ratio by factors of 2 to 5 over an interval of a few seconds are quite common. Inspection of the actual light curves reveals that spike profiles and amplitudes change substantially from one energy channel to another in an apparently random way. In Figure 3 we illustrate this variation in burst 1146, one of the flares from the A96a sample, for two channel ratios. We therefore hypothesized that these changes could be the origin of the time delays and could also be responsible for the sensitivity of the correlation analysis to the filtering and sampling interval.

To test whether amplitude variations alone can produce time delays, we simulated the data for a single channel by altering only the amplitude of one or a small number of emission spikes. We used the channel ratios to scale the spike with no changes in the timing or any other property of the data set. We then cross-correlated the simulated data against the observed data and performed the same analysis described above. For example, we used burst 1252, the light curve of which is shown in Figure 4 (*top left*) for channels 2 and 5. Notice that channel 2 has a well-defined emission spike at 80 s, but there is no corresponding spike in channel 5. There is also a rise in emission in channel 2 between 67 and 74 s with no corresponding rise in channel 5. We created simulated data by changing the amplitude of this

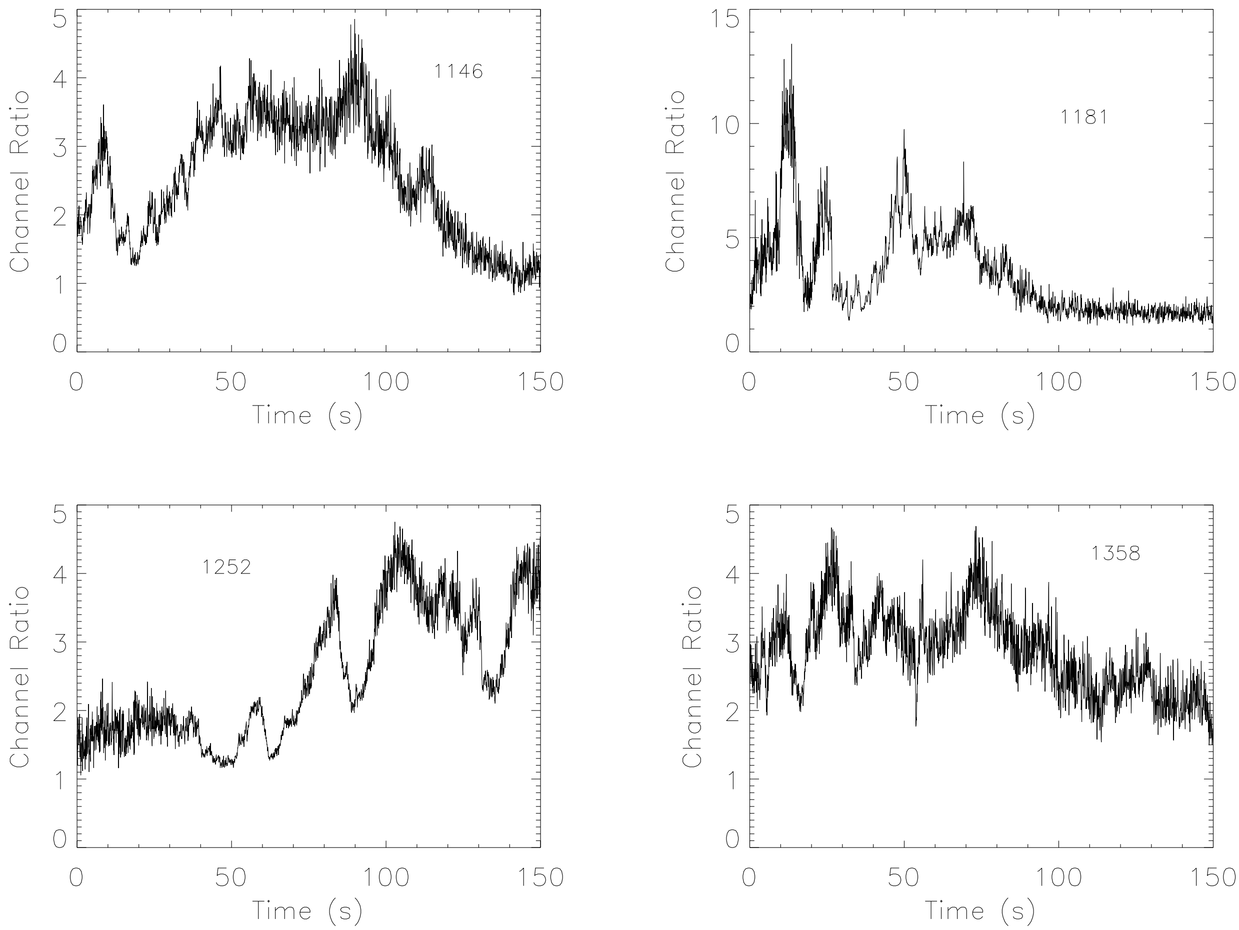

FIG. 2.—MER channel ratios. Burst 1146 (1991 December 4, start time 17:43 UT), channels 1–4 (*top left*); burst 1181, channels 4–7 (*top right*); burst 1252 (1991 December 30, start time 23:05 UT), channels 2–5 (*bottom left*); burst 1358 (1992 February 5, start time 13:16 UT), channels 2–5 (*bottom right*).

one spike as shown in Figure 4 (*top right*). We multiplied this spike by a reducing factor that flattened it to mimic the appearance of this spike in channel 5. Cross-correlating this simulated channel with the original channel 2, which is almost the same as an autocorrelation, resulted in a time delay of −49 ms. This delay has the same sign as the shift found with the real data and accounts for about one-third of the real magnitude, −159 ms. Another simulation used burst 1146, one of the original flares in A96a. We changed three spikes using the same approach. The shift obtained from the real data is +157 ms and from the simulation is +77 ms. Once again, the sign of the shift agrees, and the magnitude is no different from the observed one. In yet another simulation, using burst 1358, reducing the amplitude of *one* spike resulted in a shift of 35 ms, which is about one-fourth of the actual shift. However, increasing the amplitude of this spike beyond what is seen in the channel ratios resulted in a shift of similar magnitude but *opposite* direction! At this point we must emphasize that no criterion based on the shape of the spike or on its channel ratio biased these choices—the spikes were just typical of the flare. Since we find that positive and negative shifts can be recovered from these simulations, it is clear that changes in the spectral index can certainly account for the reported time delays.

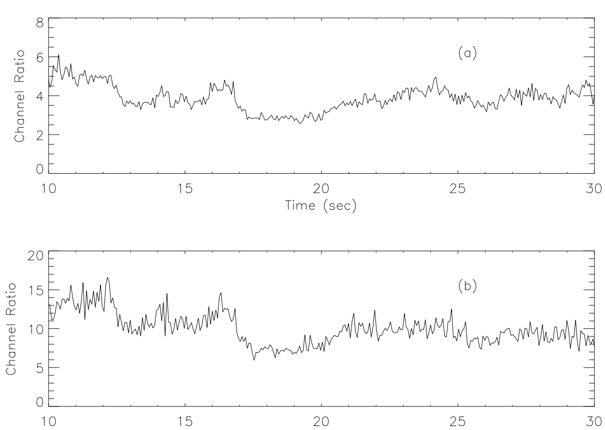

FIG. 3.—Sample high time resolution MER channel ratios. Burst 1146 (1991 December 4, start time 17:43 UT), channels 3–6 (*top*); channels 3–7 (*bottom*).

3. DISCUSSION

We have shown in this paper that small changes in individual emission spikes that mimic a change in the spectral index can significantly affect the cross-correlation of different energy channels. In particular, *altering the amplitude or shape of a single spike can change the resulting time delay by 50% to 100%*. There seem to be no systematics to the short-duration spectral index variations within any flare. The channel ratios vary considerably on timescales as short as a few seconds. Although the variability in the channel ratios

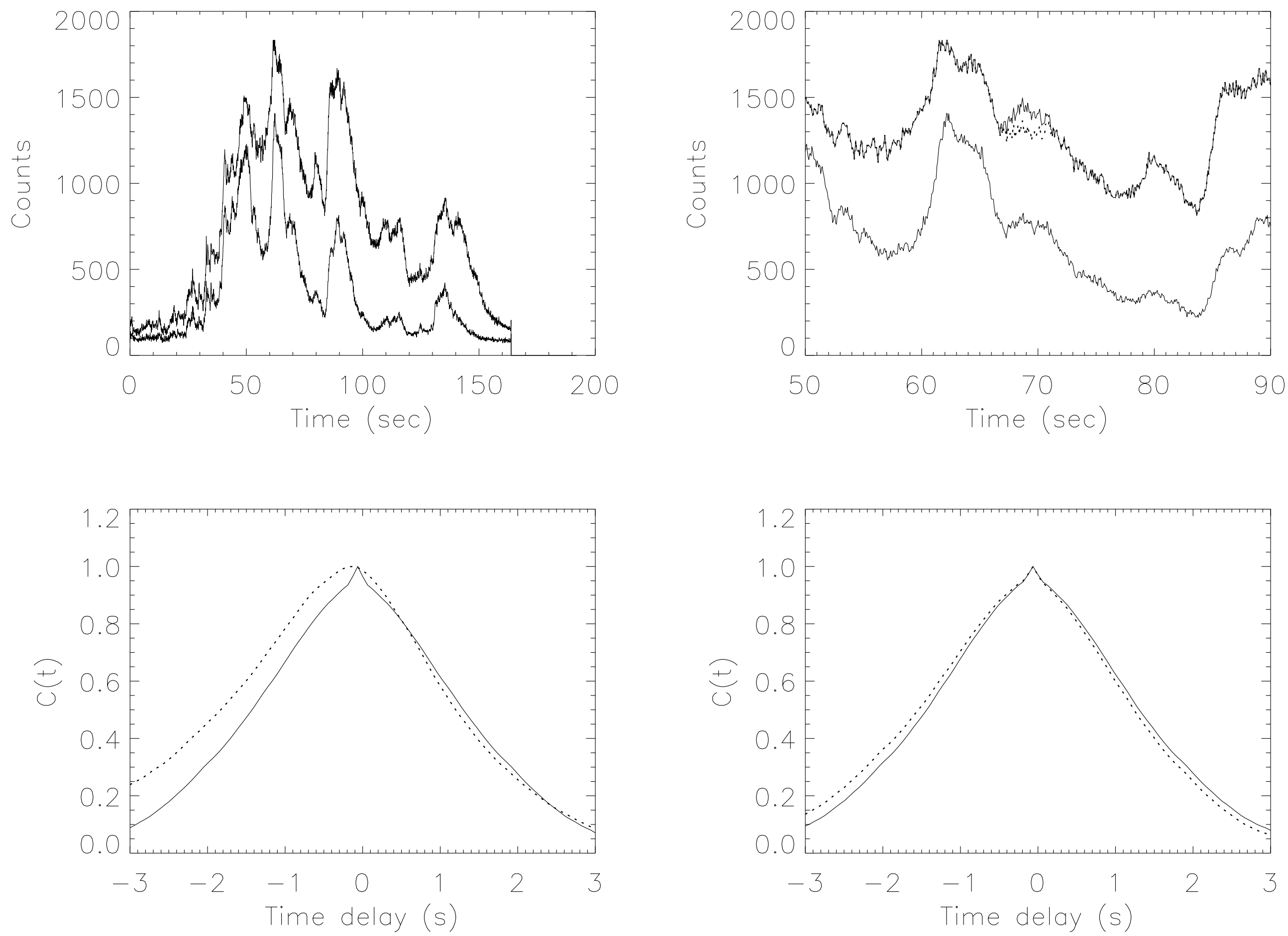

FIG. 4.—Test of dependence of time delays on small amplitude changes (see § 2.3). Burst 1252, channels 2 and 5 in the real data (*top left*); MER data for channels 2 and 5 (*solid line*) and simulated data formed by altering spike between 68 and 71 s (*top right*, *dashed line*); autocorrelation function for residuals of MER channel 2 (real data; *bottom left*, *solid line*) and the cross-correlation of residuals for MER channels 2 and 5 (*bottom left*, *dashed line*). The shift is −159 ms (see text). Autocorrelation function for residuals of MER channel 2 (real data; *solid line*) and the cross-correlation of residuals for real vs. simulated MER channel 2 (*bottom right*, *dashed line*). The shift is −49 ms (see text).

shown in Figures 2 and 3 is dramatic, it is by no means unique. This randomness of structure is further highlighted by the result that the derived shift is *very* sensitive to small changes in the size and selection of the interval used for the correlation analysis. If the derived shifts are dependent on the points used in the analysis, then a global physical effect cannot be the cause of the shift.

3.1. *Comparison with Previous Studies*

The large differences between our results and those of A96a shown in Table 1 are likely due to differences in filter width. In A96a the smoothly varying component of the emission, i.e., the envelope, is attributed to trapped electrons, and the fast timescale variations, i.e., the emission spikes, are attributed to directly precipitating electrons. The trapped electrons have the opposite time delay from the precipitating ones since the trapping time increases with energy. The timing of the smoothly varying emission therefore competes with the timing of the spikes. The authors refer to this as the "two-component model." To separate these effects, A96a chose a filter width that *maximizes* the time delay between energy channels.

If the envelope emission is due to trapped electrons, then the cross-correlation of the envelopes should result in negative time delays, i.e., low-energy envelopes should lead those at high energy because the trapping time increases with energy. Two out of the six flares shown in A96a show positive envelope shifts. This already contradicts the assertion that such shifts are always negative. We find that out of eight flares (bursts 1358, 1252, 215, 1180, 2085, 1043, 2246, and 1170), in addition to those reported in Table 1, only one flare (burst 1170) showed the high-energy envelopes lagging behind the low-energy ones. We, consequently, find no support from these data for the two-component model. Furthermore, the low-energy spike emission leads the high-energy spikes in six of the eight cases. Our results are in disagreement with the model assumptions used by A96a.

The TOF explanation relies for its verification on a systematic effect in the data—the envelope must lag relative to the spikes (Aschwanden & Schwartz 1996). In order to achieve consistent separation between the envelope and short timescale spikes, the published analyses force the time delay to be positive by choosing the filter width that maximizes the shift based on a specific interpretation of the two emission components. These alterations introduce a bias into the analysis and lead to a circular result—the shifts are in the right direction because the procedure has been tailored to support the hypothesis.

4. CONCLUSIONS

The simplest explanation for the sensitive behavior of the correlation method to filter width and interval is that the spectral variations through the flare are random, especially from one spike to another. If these short-duration changes are uncorrelated, then trimmed data sets can be easily biased by the elimination or alteration of only a few spikes. This accounts for the results from our numerical experiments. In the real data, small excesses of one skew in spike profile over its opposite can easily produce the observed shifts. We are currently developing methods to quantify this conjecture using a larger sample of BATSE flare data.

It is not possible to separate the effects of electron propagation from processes connected with the particle acceleration using correlation methods. Consequently, the assertion that the time delays between energy channels are uniquely due to electron TOF propagation is not correct.

Our aim here is to point out that this alternate interpretation of the energy-dependent time delays opens a new diagnostic possibility for analyzing these flares. Previous work has concentrated on obtaining the geometry of the flare site from the BATSE data. We suggest instead that the spectral index variations are more fundamental characteristics of the acceleration process.

We thank Markus Aschwanden for several important discussions and comparisons of methods. We also thank Richard Schwartz for assistance with the MER data and Candace Zollistch for technical support. T. N. L. was supported by a NASA JOVE grant to Kennesaw State University.

REFERENCES

Aschwanden, M. J., Hudson, H., Kosugi, T., & Schwartz, R. A. 1996, ApJ, 464, 985
Aschwanden, M. J., Kosugi, T., Hudson, H. S., Wills, M. J., & Schwartz, R. A. 1996a, ApJ, 470, 1198
Aschwanden, M. J., & Schwartz, R. A. 1996, ApJ, 464, 974
Aschwanden, M. J., Wills, M. J., Hudson, H. S., Kosugi, T., & Schwartz, R. A. 1996b, ApJ, 468, 398
Hirayama T. 1974, Sol. Phys., 34, 323
Kopp, R. A., & Pneuman, G. W. 1976, Sol. Phys., 50, 85
LaRosa, T. N., Shore, S. N., & Zollitsch, C. 1997, BAAS, 29, 01.64
Miesch, M. S., & Bally, J. 1994, ApJ, 429, 645
Miller, J. A., et al. 1997, J. Geophys. Res., 102, 14631
Sturrock, P. 1966, Nature, 211, 695
Tsuneta, S. 1996, ASP Conf. Ser. 111, Magnetic Reconnection in the Solar Atmosphere, ed. R. D. Bentley & J. T. Mariska (San Francisco: ASP)